Association for Information and Image Management
1100 Wayne Avenue, Suite 1100
Silver Spring, Maryland 20910
301/587-8202

Centimeter

1 2 3 4 5 6 7 8 9 10 11 12 13 14 15 mm

1 2 3 4 5

Inches

MANUFACTURED TO AIIM STANDARDS
BY APPLIED IMAGE, INC.

1 of 1

Photoluminescence Determination of Valence-Band Symmetry and Auger-1 Threshold Energy in Biaxially Compressed InAsSb Layers

S. R. Kurtz, R. M. Biefeld, and L. R. Dawson
Sandia National Laboratories, Albuquerque, NM 87185

Abstract: InAsSb/InGaAs strained-layer superlattices (SLSs) and InAsSb quantum wells, both with biaxially compressed InAsSb layers, were characterized using magneto-photoluminescence and compared with unstrained InAsSb and InAs alloys. In heterostructures with biaxially compressed InAsSb, the holes exhibited a decrease in effective mass, approaching that of the electrons. Correcting the data for the magneto-exciton binding energy, we obtain electron-hole reduced mass values in the range, μ=0.010-0.015, for the InAsSb heterostructures, whereas μ=0.026 and μ=0.023 for unstrained InAsSb and InAs alloys respectively. In the 2-dimensional limit, a large increase in the Auger-1 threshold energy accompanies this strain-induced change in valence-band symmetry. Correspondingly, the activation energy for nonradiative recombination in the SLSs displayed a marked increase compared with that of the unstrained alloys

1. Introduction

Frequently, the Auger-1 process (i.e. An electron and hole recombine by scattering a second electron up into the conduction band.) dominates radiative recombination in narrow bandgap III-V semiconductors, and as a result, the wavelength of diode lasers operating at room temperature has been limited to ≤ 2.1-2.3 µm.[1] In a biaxially compressed III-V layer, the |3/2,±3/2> hole ground state can increase the in-plane, electron-hole effective mass ratio (m^*_e/m^*_h) over that found in bulk material. In the 2-dimensional limit, this effective mass ratio will result in an increased threshold energy for Auger-1.[2-4] Therefore, midwave infrared (2-6 µm) emitters with biaxially compressed, InAsSb active regions may exhibit improved performance and higher temperature operation.[5] In this paper, we will describe the optical characterization of InAsSb/InGaAs strained-layer superlattices (SLSs) and InAsSb quantum wells with InAs barriers. We present evidence indicating that a large increase in Auger-1 threshold energy results from the strain-induced valence-band symmetry of the InAsSb layer.

2. Experimental Details

InAsSb and InGaAs alloys and heterostructures were grown by metal-organic chemical vapor deposition (MOCVD) on InAs substrates. SLS and ternary compositions, layer thicknesses, and lattice constants were determined from both (004) and (115) or (335) x-ray rocking curves. In this study, photoluminescence spectra for an InAsSb/InGaAs SLS and InAsSb quantum wells with InAs barriers are compared with those for unstrained $InAs_{0.93}Sb_{0.07}$ and InAs alloys. The SLS characterized in this study was an $InAs_{0.91}Sb_{0.09}$ / $In_{0.87}Ga_{0.13}As$ SLS (90 Å/ 130 Å layer thicknesses), nominally lattice matched to the InAs substrate. The multiple quantum well sample consisted of 318, 159, 106, and 53 Å thick quantum wells of $InAs_{0.91}Sb_{0.09}$, separated by 500 Å thick, InAs barriers. The sum of the four quantum well thicknesses is less than the critical layer thickness (≈ 1000 Å), and the quantum wells are psuedomorphic.

Throughout our studies of As-rich, InAsSb (5-50% Sb), the bandgaps of our InAsSb alloys were smaller than accepted values.[6] Electron diffraction results indicate compositional ordering and phase separation may occur in the As-rich, InAsSb grown at low temperatures by vapor phase epitaxy.[7] As demonstrated in the following discussion, the InAsSb material displays "single phase, random-alloy-like" optical properties except for the bandgap anomaly, and we assume that the strain imposed by the InAs heterostructure dominates any internal strain occurring within domains of the InAsSb.

Midwave infrared photoluminescence was measured by operating an FTIR in a double-modulation mode. In the magneto-photoluminescence experiments, a fluoride optical fiber was used to transmit infrared light in the magnet cryostat. The photoluminescent light was collected by the fiber and analyzed with the FTIR equipped

DISCLAIMER

with an InSb photodiode. All measurements were made in the Faraday configuration with the magnetic field parallel to the growth, (001), direction of the sample.

3. Magneto-Photoluminescence

Low temperature, zero-field photoluminescence spectra for the multiple quantum well, SLS, unstrained InAsSb, and InAs samples are shown in Figure 1. For each sample, the photoluminescence spectra consists of a single peak with a linewidth of approximately 10 meV. Emission from single quantum wells is clearly resolved in Fig 1(c), with the quantum well thickness indicated in the figure. The photoluminescence energies of the thick (318 Å) quantum well and the InAsSb alloy provide estimates of the bandgap energies of the MOCVD alloys, and both samples exhibit the bandgap anomaly. A large quantum size shift is observed for the quantum wells. Analysis of quantum size effects for InAsSb/InGaAs and InAsSb/InAs heterostructures indicates that both have type I band offsets. The bandgap and conduction band offset are sensitive to ordering or phase separation occurring in the InAsSb; the valence band offset is insensitive to these effects.

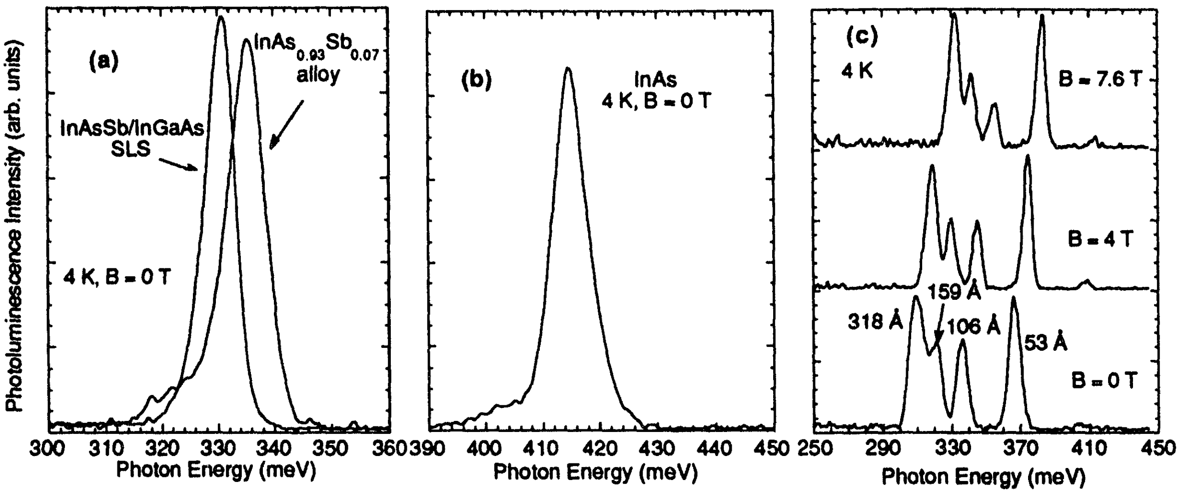

Figure 1 - Photoluminescence spectra of (a) $InAs_{0.91}Sb_{0.09}$ / $In_{0.87}Ga_{0.13}As$ SLS and $InAs_{0.93}Sb_{0.07}$ alloy, (b) InAs, and (c) $InAs_{0.91}Sb_{0.09}$/InAs quantum wells.

The magnetic field dependence of the photoluminescence energies for each of these samples is shown in Figure 2. For each photoluminescence line, the reduced mass, μ, corresponding to the slope obtained from the free electron-hole approximation ($\frac{dE}{dB} = \mu_B\left(\frac{1}{m_e^*}+\frac{1}{m_h^*}\right) = \frac{\mu_B}{\mu}$; μ_B is the Bohr magneton), is indicated in the figure. The reduced masses for the unstrained alloys (μ_{InAsSb}= 0.037 and μ_{InAs}=0.031, in units of free electron mass) are significantly larger than those observed in the strained heterostructures (μ=0.015-0.024) due to the low in-plane hole mass associated with the heavy-hole ($|3/2,\pm 3/2\rangle$) ground state of the biaxially compressed, InAsSb layers.

Excitonic behavior is revealed in the magneto-photoluminescence results. For all samples, the photoluminescence peak energy is insensitive to magnetic field for B< 2T, characteristic of a diamagnetic exciton, and in the linear region observed at higher fields, the reduced mass values obtained from the free carrier approximation are consistently too large, due in part to the binding energy of the exciton. Also, note the increase in reduced mass (or decrease in slope) as the quantum wells become thinner (Fig. 2(b)).

Using measured parameters for InAs and semi-empirical expressions for nonparabolicity and magneto-exciton energies, we can estimate exciton binding energies and correct the reduced mass values.[8] Assuming a 3-dimensional exciton, we obtain corrected reduced mass values, μ=0.010, 0.026, and 0.023, for the 318 Å thick quantum well, unstrained InAsSb alloy, and InAs, respectively. The exciton binding energies for the 318 Å well and the alloys were 1.0 meV and 1.8 meV, respectively. Examining the thinnest (53 Å) quantum well, we estimate an exciton binding energy of 3-4 meV for a band minimum reduced mass, μ=0.010, and assuming a 2-dimensional exciton. The change in slope in Fig 2(b), associated with quantum confinement, indicates an increase in exciton binding energy of the correct magnitude.[8]

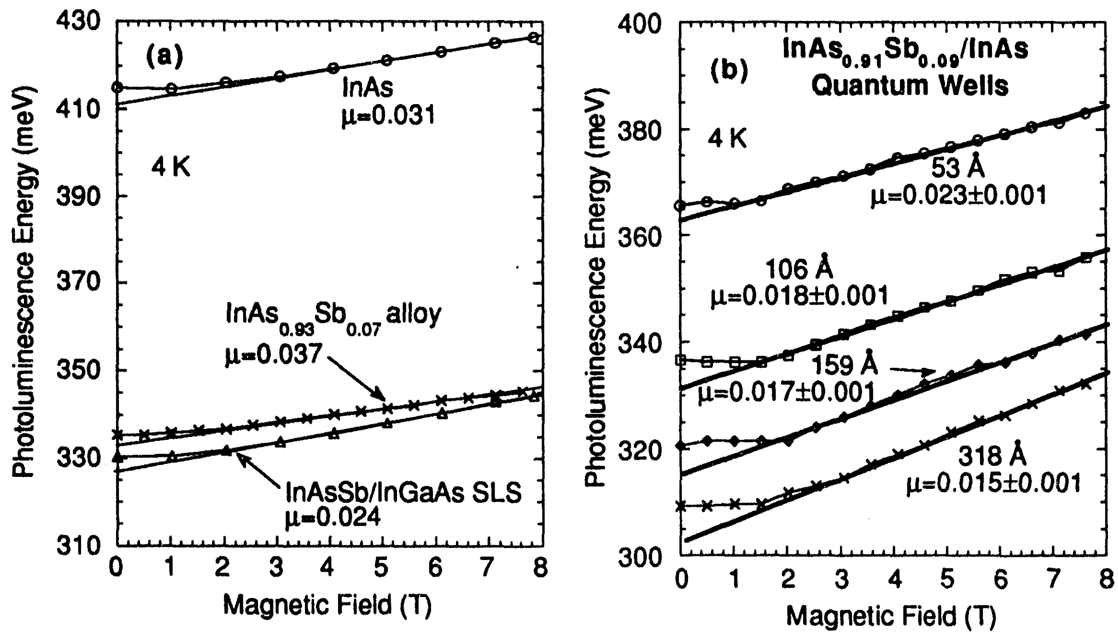

Figure 2 - Magnetic field-induced shift of the photoluminescence energy for (a) the InAsSb/InGaAs SLS and the InAsSb and InAs alloys, and (b) the InAsSb/InAs quantum wells.

4. Modification of Auger-1 Threshold Energies

In the 2-dimensional limit, a large increase in the Auger-1 threshold energy accompanies this strain-induced change in valence-band symmetry. We examined the temperature dependence of the photoluminescence intensity for SLS and bulk, $InAs_{0.93}Sb_{0.07}$ and InAs samples. (see Figure 3) At > 100 K, the radiative efficiency decreases exponentially for all samples, and the activation energy for nonradiative recombination (ΔE) in the SLS displayed a marked increase compared with that of the unstrained alloys (ΔE=0.26 E_{gap} vs ΔE=0.06 E_{gap}). Other InAsSb/InGaAs SLSs that we examined also displayed large activation energies. Due to variations in optical alignment and sample doping and defects, the differences in the relative radiative efficiency between samples may not be accurate.

Approaching room temperature, Auger-1 will be the dominant nonradiative process. The radiative efficiency is

$$\eta = \frac{\tau_A}{\tau_R} \propto \left(1/n_0\right) \cdot \exp\left(\frac{\Delta E}{kT}\right) \quad (1) \qquad \text{and} \qquad \Delta E = \left(\frac{m_e^*/m_h^*}{1+\left(m_e^*/m_h^*\right)}\right) \cdot E_{gap} \quad (2),$$

where n_0 is the electron density, $\tau_R \propto \left(n_0/T^{3/2}\right)^{-1}$ is the radiative lifetime, and $\tau_A \propto \left(T^2/n_0^2\right)\exp(\Delta E/kT)$ is the Auger-1 lifetime.[9] Eq. 1 is based on simple energy-momentum conservation for isotropic, parabolic bands, and the expression for activation energy, ΔE (ΔE = Auger threshold - Bandgap), is valid in 2 or 3-dimensions.[2] In the 2-dimensional limit, the SLS in-plane effective masses determine ΔE,[3,4] and therefore, the SLS activation energy is larger than that of the unstrained alloys due to the decreased hole mass in biaxially compressed layers of the SLS.

Electron-hole effective mass ratios for each sample are compared with theoretical values obtained from k·p calculations and with experimental values obtained from magneto-photoluminescence and temperature dependence studies. In each case there is good agreement between theoretical and experimentally determined mass ratios. The effective mass ratios (m^*_e / m^*_h) determined by the 3 methods for the SLS were in the range, 0.3-0.5, and the effective mass ratios for the unstrained alloys were 0.06±0.02.[9] Comparing the SLS with the alloys, the SLS consistently displayed the predicted effects of the valence band under biaxial compression.

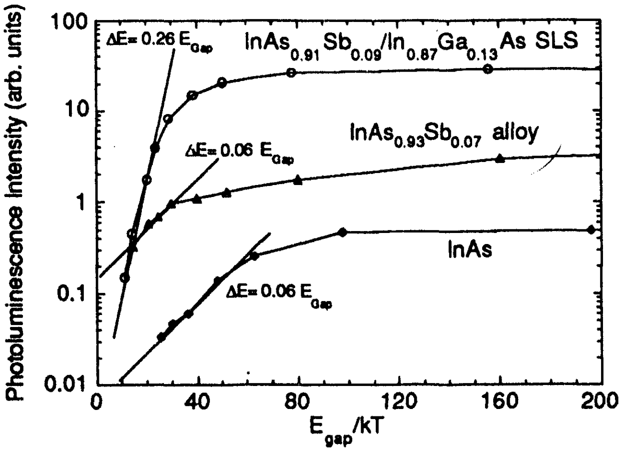

Figure 3 - Temperature dependence of the photoluminescence intensity (radiative efficiency) for the InAsSb/InGaAs SLS and InAsSb and InAs alloys. Activation energies (ΔE) are indicated in the figure.

5. Conclusions

Using infrared photoluminescence and magneto-photoluminescence, we have examined the electronic properties of a series of heterostructures with biaxially compressed InAsSb. Holes are confined to the heavy hole (small in-plane effective mass) ground state of the biaxially compressed InAsSb layers, and the band offsets for these heterostructure are type I. Analysis of the magneto-excitonic behavior indicates that the hole mass may be quite small (μ=0.010), and exciton binding energy increases with quantum confinement. The photoluminescence efficiency versus temperature revealed that an increased activation energy for nonradiative recombination accompanies the decreased hole mass in the SLS. Photoluminescence efficiency activation energies for the SLS and unstrained alloys agree with predicted Auger-1 threshold energies, with the activation energy for the SLS approaching the Auger-1 value in the 2-dimensional limit. Although the material properties of the MOCVD-grown InAsSb are non-ideal, these heterostructures display Auger-1 threshold energies, effective masses, band offsets, and "random alloy-like" properties that are desirable for active regions in midwave infrared diode lasers.

J. A. Bur, K. C. Baucom, and M. W. Pelczynski provided technical assistance. This work was performed at Sandia National Laboratories, supported by the U. S. Department of Energy under contract No. DE-AC04-94AL85000.

References

1. S. J. Eglash and H. K. Choi, Appl. Phys. Lett. 57,1292 (1990); 61 1154 (1992).
2. N. K. Dutta, J. Appl. Phys. 54, 1236 (1983).
3. A. R. Adams, Elect. Lett. 22, 249 (1986).
4. E. Yablonovich and E. O. Kane, IEEE J. Lightwave Tech. 6, 1292 (1988).
5. S. R. Kurtz, R. M. Biefeld, L. R. Dawson, K.C. Baucom, and A. J. Howard, Appl. Phys. Lett. 64, 812 (1994).
6. Z. M. Fang, K. Y. Ma, D. H. Jaw, R. M. Cohen, and G. B. Stringfellow, J. Appl. Phys. 67, 7034 (1990), and references therein.
7. D. M. Follstaedt, R. M. Biefeld, K. C. Baucom, and S. R. Kurtz (submitted to J. Elect. Mat.).
8. S. R. Kurtz and R. M. Biefeld (submitted to Appl. Phys. Lett.).
9. S. R. Kurtz, R. M. Biefeld, and L. R. Dawson (accepted for publication, Appl. Phys. Lett.).

DATE
FILMED
10/13/94

END